Compact Raman Lidar (CRL) Water Vapor and Temperature Measurements During CHEESEHEAD

Zhien Wang, Professor
University of Colorado, Boulder
Laboratory for Atmospheric and Space Physics
Department of Atmospheric and Oceanic Sciences
3665 Discovery Dr.
Boulder, CO 80303-7819
Phone: 303-492-1613 (office)
zhien.wang@colorado.edu
ORCID: 0000-0003-3871-3834

1.0 Data Set Overview:

Compact Raman Lidar (CRL) measurements of water vapor and temperature profiles from the University of Wyoming King Air (UWKA) during CHEESEHEAD IOPs are provided. The three IOP periods are July 9-13, Aug 20-23, and Sep 24-29. During these IOPs, UWKA conducted pre-defined cross-wind legs at ~400 m and 100 m the ground around the central tall tower site (45.9459, -90.2723; 470 m). Due to the limitations of CRL overlaps, data from 100m legs are challenging to process. Thus, only water vapor and temperature profiles from the 400-m legs are archived here.

2.0 Instrument Description:

The CRL is the first Raman lidar system developed for use on the UWKA. It uses a compact, lightweight transmitting-receiving system. As illustrated in Fig. 1, the CRL integrated telescope, laser, and receiving system fits into a box of 13x20x26 inches weighing approximately100 lbs. The CRL was initially developed to obtain 2-D distributions of water vapor, aerosols, and clouds and was first deployed on the UWKA in 2010 (Liu et al. 2014). In early 2015, low-J and high-J pure rotational Raman channels (J is the rotational quantum number) were added to provide temperature measurements (Wu et al. 2016). Table 1 lists the specifications of CRL. Although low laser energy (50-mJ) limits water vapor measurement to short-range under high solar background conditions, the CRL still can provide excellent data for characterizing the spatial variability of aerosol, water vapor, and temperature. In general, CRL water vapor and temperature measurement accuracies depend on the range and averaging, as discussed in section 3.

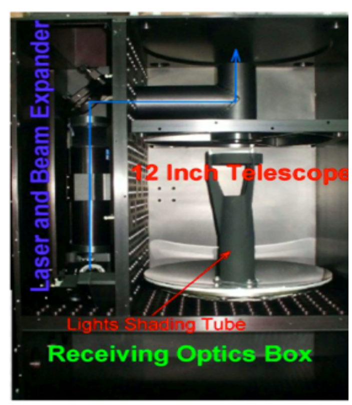

Figure 1. Photograph of CRL inner structure.

Table 1. Main system parameters of CRL and MARLi including the Normal Ocular

Hazard Distance (NOHD)

	CRL
Laser	Bigsky CFR 400 GRM
Wavelength (nm)	354.7
Pulse Energy and width	50 mJ and 9 ns
Repetition Rate (Hz)	30
Beam Expander	5x
Telescope (Cassegrain)	
Size (inch)	12
Field of View (mrad)	1
Receiving System	
Channel Number	5
Detector (PMT)	Hamamatsu H10720
Data Acquisition	NI 16-bit, 250 MHz A/D card
NOHD (meters)	< 200

3.0 Data Collection and Processing:

During CHEESEHEAD IOPs, UWKA conducted morning and afternoon flights (~3.5 hours) under non-precipitation days. Thus, UWKA in situ and CRL data capture daytime PBL evolutions. According to the mean wind directions, a pre-defined cross-wind flight pattern will be selected for a given flight. Each flight collected data at 100m and 400 m stacked legs, as illustrated in Fig. 2.

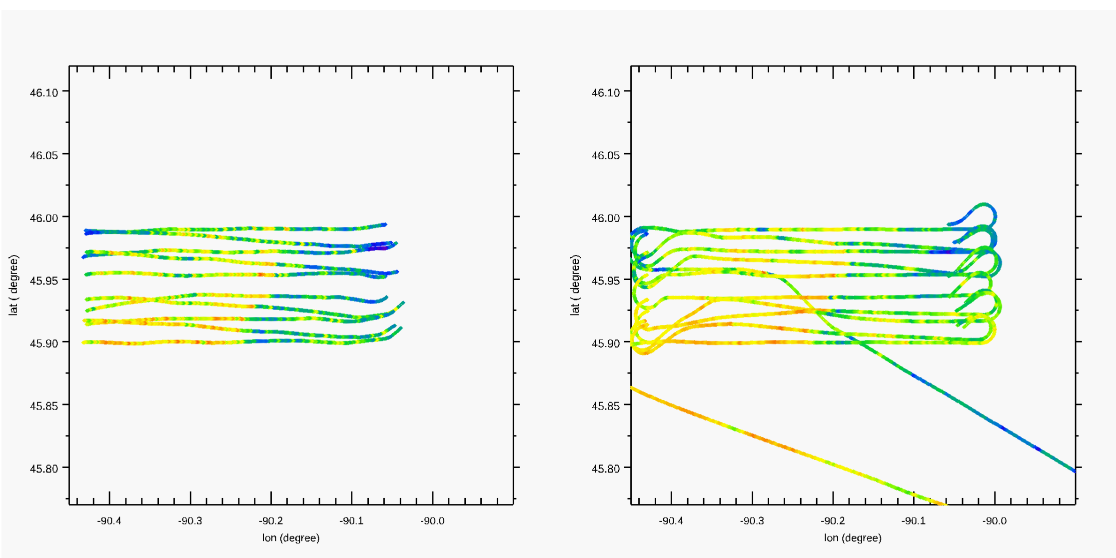

Figure 2. An example of 100m (left) and 400 m (right) legs for the July 11 afternoon flight. The color indicates flight level water vapor variations based on in situ measurements.

CRL data processing involves three critical aspects: near range overlap correction, averaging, and calibration. Because of slightly different near range overlap functions among channels, we need to correct their differences for water vapor and temperature determinations. To achieve the overlap correction goal, stacked leg measurements within homogeneous PBL and above 1000 m were collected to evaluate near range overlap corrections for water vapor and temperature, as illustrated in Wu et al. (2016). For CHEESEHEAD data, only near-range overlap correction for temperature is applied. The overlap corrections introduce significant uncertainties for measurements within 100 m of the flight level; thus, only CRL data at 400-m legs are provided here.

Realtime CRL data were recorded at 10 Hz and 0.6 m vertical resolution. A 9-s horizontal and 45 m vertical moving averaging is applied for the post data processing. Before the averaging, surface/treetop detections were performed. To avoid surface contamination, the averaging is only applied to signals above the surface; thus, the near-surface has less averaging in the current processing. "Leefilt" (an IDL routine, Lee 1986) is applied for further vertical smooth.

Calibrations for water vapor and temperature are done by comparing CRL near range measurements with flight-level in situ measurements. For water vapor, one calibration was applied to the whole project. For temperature measurements, we have to apply time-dependent calibration draft corrections due to cabin temperature variations.

Three observations examples are provided in Fig. 3. Within each panel, the black region indicates the canopy or the ground. CRL can provide canopy top or the surface heights at 0.6 m, which can be provided if it is useful for any studies. Aerosol distribution is provided as lidar scattering ratio (LSR), which is defined as the ratio of total backscattering to molecular backscattering. However, we didn't collect free troposphere data to provide aerosol free data reliably calibrate LSR during the campaign. Thus, provided LSR is not well calibrated, but related LSR variations can be used to study the relative variations of aerosols. For example, there are noticeable spatial aerosol variations in case *a* and precipitation detected at the end of the leg in case c. CRL water vapor mixing ratio (WVMR, g/kg) can resolve significant water vapor variations with PBL. For the case *a*, coherent water vapor and aerosol variations can be noticed. Cases *b* and *c* present consistent temperature and water vapor variations. For the case *b*, the temperature inversion layer at 300-400 m above the ground is evident and consistent with the water vapor gradient. During the case c, a storm with light precipitation was moving into the sampling region, which generated higher WVMR and colder temperature for the second half of the leg than the first half.

a) For aircraft.UWyo_King_Air.20190709_152542_153123.CRL.cdf

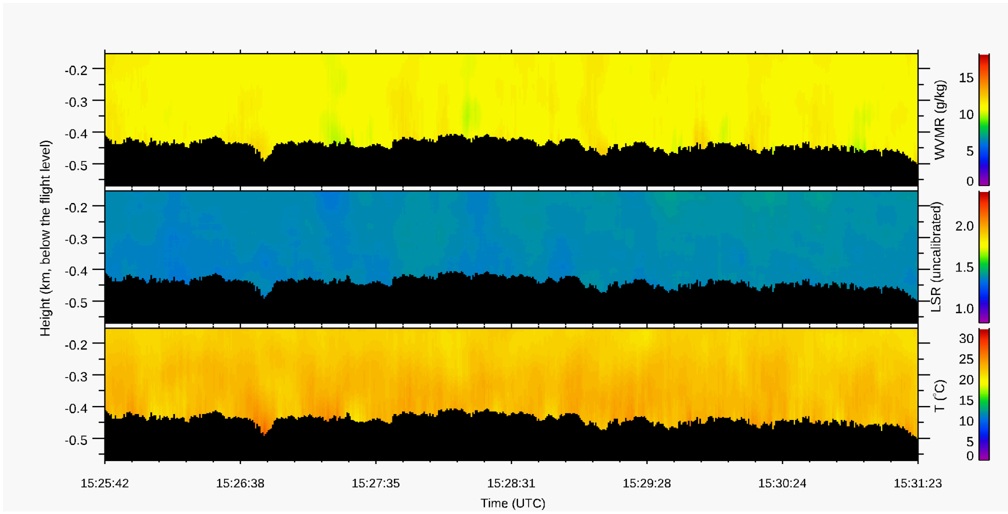

b) For aircraft.UWyo_King_Air.20190820_140619_141139.CRL.cdf

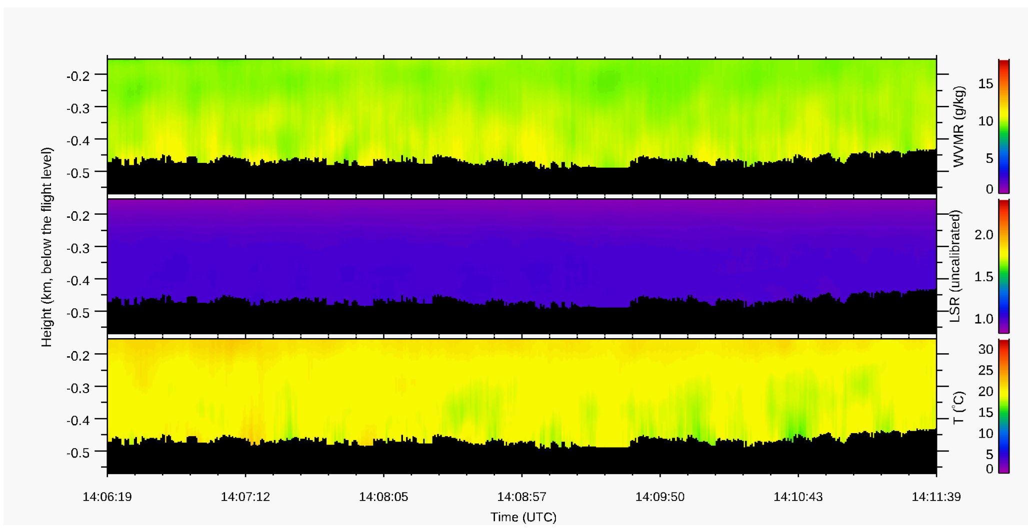

c) For aircraft.UWyo_King_Air.20190820_151801_152142.CRL.cdf

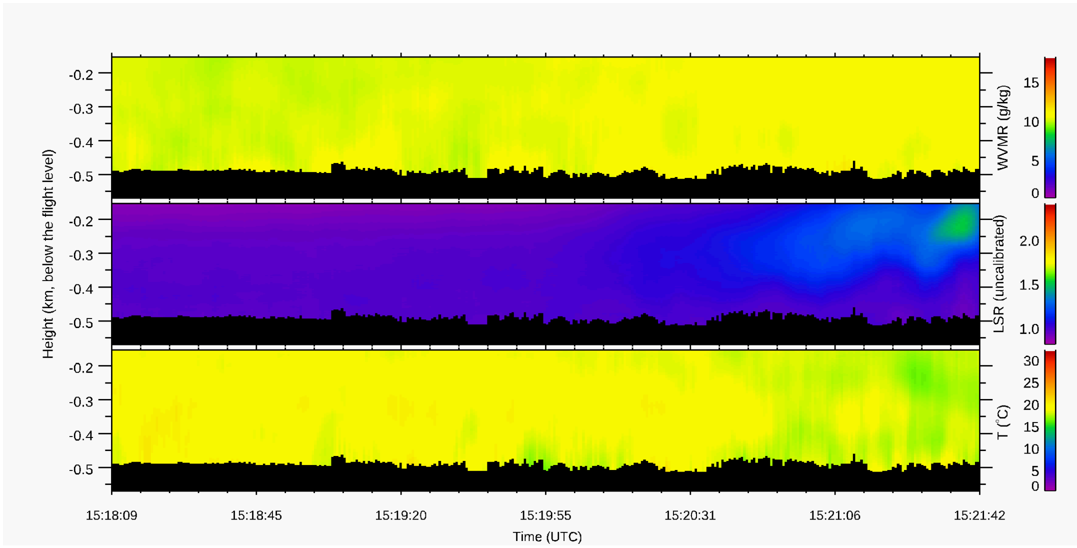

Figure 3. Examples of 400 m leg CRL measurements on July 9th and August 20th. For each leg, CRL provides vertical profiles of water vapor mixing ratio (WVMR, top), aerosol LSR (middle), and temperature (bottom).

The stacked 400 m and 100 m flight legs offer a unique data set to evaluate CRL water vapor and temperature measurements. Figure 4 compares CRL measurements at 120 m below the flight level and at the mean 100m leg level with in situ measurements. The results show that CRL and in situ temperature and water vapor measurements are highly correlated with mean temperature and water vapor differences of 0.7K and 0.17 g/kg. These low mean differences indicate reliable CRL measurements, especially considering the spatial/temporal variability of water vapor and temperature.

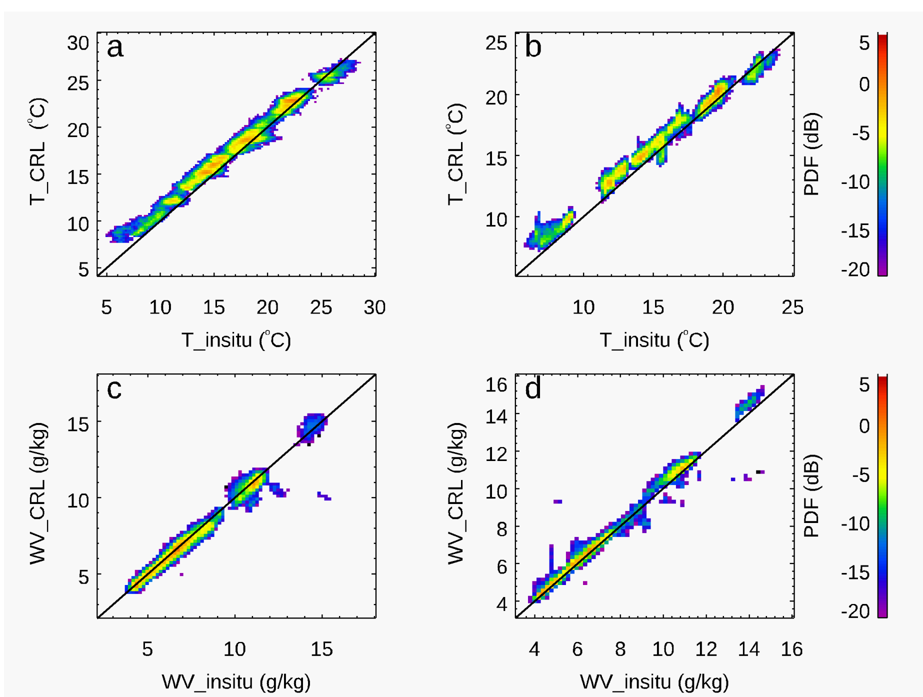

Figure 4. Inter-comparison of CRL and in situ measurements of water vapor and temperature. Figures a and c are for results at the low level leg, and figures b and d are for the high legs.

4.0 Data Format:

CRL Data for each flight leg is saved into a NETCDF file, which contains related information for each variable. Other than CRL data, UWKA flight location and altitude are provided to geo-locate CRL measurements. JPG images are also provided for each NetCDF files. Figure 3 offers a few selected examples. An IDL code (read_raman_cdf.pro) is also provided to read and plot the data.

5.0 Data Remarks:

The archived 400 m leg data are good other than two minor issues: (1) temperature calibration can be further refined; (2) the current smooth averaging for near-surface data points can be improved to provide even averaging for the full profile.

There are no missing data periods. If there are any interests in re-processing the 400m leg data for a specific period or exploring some 100m leg data, feel free to contact the instrument PI.

6.0 References:

Wu, D., Z. Wang, P. Wechsler, N. Mahon, M. Deng, B. Glover, M. Burkhart, W. Kuestner, and B. Hesen, 2016: Airborne compact rotational Raman lidar for temperature measurement. *Optics express*, **22** (17), to be submitted.

Wang, Z. et al., 2015: AIRBORNE RAMAN LIDAR AND ITS APPLICATIONS FOR ATMOSPHERIC PROCESS STUDIES, Presented at Twenty Seventh International Laser Radar Conference, July 5 - 10, 2015, New York City, NY.

Liu B., Z. Wang, Y Cai, P. Wechsler, W Kuestner, M Burkhart, W Welch, 2014: Compact airborne Raman lidar for profiling aerosol, water vapor and clouds, *Optics express*, **22** (17), 20613-20621.

Wang, Z. and Co-authors, 2011: Observations of boundary layer water vapor and aerosol structures with a compact airborne Raman lidar. 5th Symposium on Lidar Atmospheric Applications, 91st AMS Annual Meeting, Seattle

Lee, Jong-Sen, 1986: Speckle suppression and analysis for synthetic aperture radar images, Opt. Eng. 25(5), 255636, https://doi.org/10.1117/12.7973877.